

---

# Relative Young's modulus identification using elastography

Jérôme Fehrenbach<sup>†</sup> — Mohamed Masmoudi<sup>†</sup> — Rémi Souchon<sup>‡</sup> —  
Philippe Trompette<sup>‡</sup>

<sup>†</sup> Laboratoire MIP UMR 5640, 118 route de Narbonne, 31062 Toulouse cedex 4

<sup>‡</sup> Unité de recherche INSERM U556, 151 cours Albert Thomas, 69424 Lyon cedex 03

---

*RÉSUMÉ.* Certains tissus biologiques comme la prostate peuvent être considérés comme un matériau élastique linéaire et isotrope, au moins pour de petites déformations. Un problème intéressant - du point de vue médical - est de détecter des hétérogénéités où le module d'Young prend une valeur différente du reste. On se donne ici un matériau homogène sauf dans certaines régions où son module d'Young prend une valeur différente. On propose une méthode pour reconstruire une approximation du module d'Young relatif, c'est-à-dire le quotient des modules d'Young. L'outil principal est une méthode générale pour les problèmes inverses : il s'agit d'une implémentation économe en mémoire et en calculs de la méthode de Gauss-Newton, basée sur l'utilisation de la dérivation algorithmique en mode direct et en mode adjoint. Cette méthode est illustrée par des résultats expérimentaux sur un fantôme de gélatine : la propriété de régularisation de l'algorithme de Gauss-Newton permet de localiser les plus grosses hétérogénéités.

*ABSTRACT.* Some biological tissues like the prostate can be considered as a linear isotropic medium, at least for small strains. An interesting problem - from the medical point of view - is to detect heterogeneities where the Young's modulus takes a different value from the background. A homogeneous medium is considered here, except in some regions where Young's modulus takes a different value. A method is proposed to reconstruct an approximation of relative Young's modulus, that is the ratio of Young's moduli. The main tool is a general method for inverse problems: it is an implementation of Gauss-Newton's method that uses few memory and few computations, based on the use of direct and adjoint derivative. This method is illustrated with experimental results on a gelatin phantom: the regularization property of Gauss-Newton's algorithm allows to locate the larger heterogeneities.

*MOTS-CLÉS :* élastographie, imagerie médicale, optimisation topologique, problème inverse, élasticité, échographie.

*KEYWORDS:* elastography, medical imaging, topological optimization, inverse problems, elasticity, echography.

---

## 1. Introduction

Prostate and breast tumors can have a Young's modulus much higher than the surrounding safe tissue, they can be 4 to 10 or more times stiffer (Krouskop, Wheeler, Kallel, Garra et Hall 1998), this ratio is called the relative Young's modulus, or the contrast. The detection of tumors by clinical palpation requires that the hard nodulus have to be big or near enough from the skin. Elastography was introduced in (Ophir, Cespedes, Ponnekanti, Yazdi et Li 1991), it is an imaging technique that provides a strain image, called elastogram, by comparison of two sonograms before and after a small external compression. A recent review article on elastography is (Ophir, Alam, Garra, Kallel, Konofagou, Krouskop, Merritt, Righetti, Souchon, Srinivasan et Varghese 2002). Related time-dependent imaging modalities are dynamic elastography (Gao, Parker et Alam 1995), and transient elastography (Catheline, Wu et Fink 1999), we do not adress these issues here.

The inverse problem framework (Kirsch 1996) is used here to provide an image of Young's modulus distribution from an elastogram. Gauss-Newton algorithm is a regularization method for inverse problems, it chooses a perturbation of minimal norm taking into account information data from the physical model (the Jacobian matrix and its transpose) to compensate for the lack of measured data. Previous work using Gauss-Newton algorithm for Young's modulus estimation are (Kallel et Bertrand 1996), (Doyley, Meaney et Bamber 2000), and (Doyley, Srinivasan, Pendergrass, Wu et Ophir 2005), where interesting results are obtained. However, in these works a heavy computation load is required and hence only coarse meshes are used. This limits the size of the heterogeneities to be detected.

We show here that Gauss-Newton method can be implemented thanks to both forward and reverse modes of algorithmic differentiation (Griewank 2000). This implementation of Gauss-Newton algorithm has the advantage of being no more expensive than the gradient method and gives a better convergence.

In this paper, the direct problem for elasticity is recalled (section 2). We explain then (section 3) the strategy of the inverse problem : reconstructing Young's modulus from the radial displacement under known boundary conditions. The implementation of Gauss-Newton algorithm using forward and reverse modes of algorithmic differentiation is then splitted in short algorithms. In the last section, in vitro experimental results on a gelatin phantom are given.

## 2. Direct problem

Consider a smooth domain  $\Omega$  in the plane. The boundary of  $\Omega$  is divided into two parts :  $\partial\Omega = \Gamma_N \cup \Gamma_D$ . The domain  $\Omega$  is filled with an elastic material, subject to a displacement  $u \in L^2(\Omega, \mathbf{R}^2)$ . There are no volume forces, there is a known displacement  $d$  on  $\Gamma_D$  and known forces  $f$  on  $\Gamma_N$ . The Lamé coefficients of the material  $\lambda = \lambda(x) = \lambda_0 E(x)$  and  $\mu = \mu(x) = \mu_0 E(x)$  depend on the space variable (this is equivalent to assuming the Poisson ratio  $\nu$  is constant, and the Young's modulus  $E(x)$ )

depends on the space variable). In the numerical application, we will take  $\nu$  equal to 0.45 (it is the value that proved to fit the best to our measured data).

The boundary values problem is to find a displacement field  $u$  and a stress field  $\sigma$  defined in  $\Omega$  by :

$$(BP) \begin{cases} \sigma &= \lambda \operatorname{tr} \epsilon(u) I + 2\mu \epsilon(u) & \Omega \\ -\operatorname{div} \sigma &= 0 & \Omega \\ \sigma \cdot n &= f & \Gamma_N \\ u &= d & \Gamma_D \end{cases}$$

We perform a degree one finite elements method on a triangular mesh with  $n$  nodes : the finite elements version of the mixed boundary problem  $(BP)$  is equivalent to the linear system :

$$Aq = b,$$

where  $q \in \mathbf{R}^{2n}$  is the displacement vector,  $b \in \mathbf{R}^{2n}$  is defined by the boundary conditions and  $A$  is the stiffness matrix.

The stiffness matrix  $A$  depends on Young's modulus distribution  $E$ , this matrix is denoted  $A(E)$ . Note that  $E \mapsto A(E)$  is an affine map, and let  $\hat{A}$  be its linear part : for every  $E$  and every  $h$ ,  $DA(E).h = \hat{A}(h)$ .

### 3. Inverse problem

We look for heterogeneities having Young's modulus  $E_2$  in a material having Young's modulus  $E_1$ . The quantity  $E_2/E_1$  is called the contrast (or relative Young's modulus) of the heterogeneity. We will see in section 4 that the Neumann boundary conditions are not really known, but are computed up to a choice of a scaling factor. Changing this factor amounts to changing  $E_1$ . In practice, the value of  $E_1$  is taken to be 1. The known measure is the radial displacement  $u_r^{\text{measur.}}$  under known boundary conditions, and the unknown is the location of the heterogeneities and the value of the contrast.

The radial displacement at a point  $M$  is given by  $u_r = L.u$ , where  $L$  is a linear operator, called the state-to-observation operator. The  $n \times 2n$  matrix of the discretized version of this operator can be easily formed, this matrix is also denoted  $L$ .

We want to minimize the following quantity :

$$j(E) = \frac{1}{2} \|L.u_E - u_r^{\text{measur.}}\|^2 = \frac{1}{2} \|F(E)\|^2,$$

where  $F(E) = L.u_E - u_r^{\text{measur.}}$ , with  $u_E$  solution of  $A(E)u_E = b$ .

We apply Gauss-Newton algorithm, starting from an homogeneous distribution  $E \equiv E_1$  : we shall compute an iterate of Newton  $E + d$  with  $d$  solution of :

$$DF^T DFd = -DF^T F.$$

The vector  $d$  will be searched by the conjugate gradient method. Indeed, the conjugate gradient method requires only to know the product of the given matrix by a vector, avoiding thus to compute the whole Jacobian matrix, a matrix-matrix multiplication and the use of memory to store a (non sparse) matrix.

For the computation of  $DF^T DFx$  when the vector  $x$  is given, we use the algorithmic differentiation rules, and proceed as follows :

1) **Computing**  $z = DFx$

It is the directional derivative of a vectorial function : we use forward differentiation.

2) **Computing**  $DF^T z$

It is a scalar criterion : we use reverse mode of algorithmic differentiation.

**Proposition 1 (Computing  $z = DFx$ )**

$$z = L\delta$$

where  $\delta$  is solution of the linear system

$$A(E)\delta = -\widehat{A}(x)u_E,$$

where  $\widehat{A}(x) = A(x) - A(0)$ .

*proof* : Differentiate the relation  $A(E)u_E = b$ .  $\square$

**Proposition 2 (Computing  $DF^T z$ )** Let  $v_E \in \mathbf{R}^{2n}$  be the solution of the linear system

$$A^T v = -L^T z,$$

Then for any vector  $h \in \mathbf{R}^n$  :

$$(DF^T)z.h = [D(F^T z)].h = (\widehat{A}(h)u_E | v_E)$$

*proof* : Consider the Lagrangian

$$\mathcal{L}(E, u, v) = F(u)^T z + (A(E)u - b | v).$$

Then for any  $v$ ,  $F(u_E)^T z = \mathcal{L}(E, u_E, v)$  hence  $D_E(F^T z) = D_1 \mathcal{L}(E, u_E, v) + D_2 \mathcal{L}(E, u_E, v).D_E u_E$ .

Take  $v = v_E$  satisfying  $A^T v_E = -L^T z$  so that the second term above vanishes, and obtain  $(DF^T)^T.z.h = D(F^T z).h = D_1 \mathcal{L}(E, u_E, v_E).h = (\widehat{A}(h)u_E | v_E)$ .  $\square$

**Corollary 1 (Computing  $DF^T F$ )** Let  $w_E \in \mathbf{R}^{2n}$  be the solution of the linear system

$$A^T w = -L^T F, \quad (*)$$

Then

$$\forall h \in \mathbf{R}^n, \quad (DF^T)F.h = (\widehat{A}(h)u_E | w_E).$$

**Algorithm 1 :** Finding the Young's modulus distribution :

- input :** *mesh*,  $E_1$ ,  $\nu$ , *boundary conditions*,  $u_r^{\text{measur.}}$
- construct the matrix  $L$  from mesh data,
  - compute the stiffness matrix  $A$  assuming homogeneous Young's modulus  $E \equiv E_1$ , compute the direct state  $u_E$ ,
  - compute the adjoint state  $w_E$  using (\*),
  - compute  $DF^T F$  using corollary 1,
  - solve for  $d$  the equation  $DF^T DFd = -DF^T F$  using the conjugate gradient method, the multiplication of a vector by  $DF^T DF$  is given by algorithm 2,
  - the estimated Young's modulus distribution is  $E + d$ .

**Algorithm 2 :** Computing  $y = DF^T DFx$  for a given vector  $x$

- input :** *mesh*,  $\nu$ , *stiffness matrix*  $A(E)$ , *direct state*  $u_E$ , *matrix*  $L$
- solve for  $\delta$  the equation  $A(E)\delta = -\hat{A}(x)u_E$ ,
  - compute  $z = L.\delta$  (see proposition 1),
  - solve for  $v_E$  the equation  $A^T v_E = -L^T z$ ,
  - the components ( $y_i$ ) of  $y$  are given by  $y_i = (A(e_i)u_E|v_E)$  (see proposition 2).

#### 4. Experimental results

We applied the algorithm above to experimental data (Souchon, Soualmi, Bertrand, Chapelon, Kallel et Ophir 2002). This experiment was designed to demonstrate the feasibility of generating an image of the modulus contrast experimentally in a phantom. The imaging system is based on an ultrasound scanner (Combison 311, Kretz, Austria) equipped with a transrectal probe (IRW 77AK, Kretz, Austria). The probe was covered by a latex balloon filled with a coupling liquid that ensured good acoustic coupling between the probe and the phantom. A hollow cylindrical phantom of gelatin was prepared. It contained six stiff foam inclusions of length 8cm, width 1cm and various thicknesses, ranging from 0.55 to 2.6mm (see fig.1). The hollow phantom was immersed in water, but it was left free to move (but for pins at some points) : during the inflation sequence, it moved a little to the right (relatively to the probe).

The phantom was compressed by inflating the balloon : the measures are the radial displacements between before and after inflation, see (Souchon, Rouvière, Gelet, Detti, Srinivasan, Ophir et Chapelon 2003) for details about data acquisition and strain estimation. At every point of the domain, the measured data is the radial displacement. When differentiating this radial displacement along the rays, one obtains a strain elastogram that is shown on figure 2. On the strain elastogram, the inclusions are visible, but the contrast of Young's modulus can not be estimated.

The data are treated as follows :

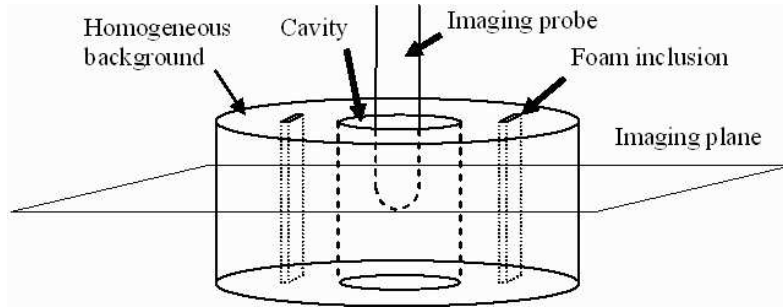


**Figure 1.** Experiment setup. The tip of the imaging probe is covered by a balloon that fills the whole cavity once it is inflated.

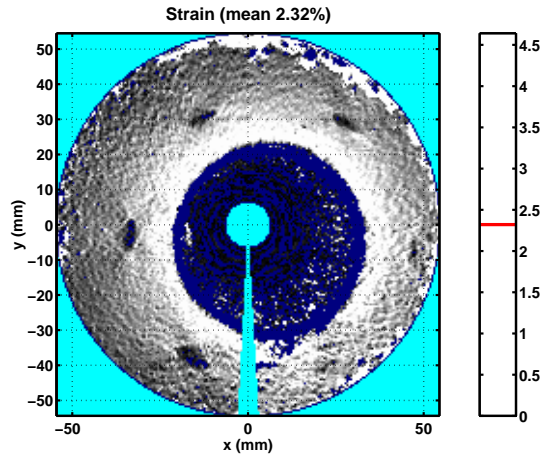


**Figure 2.** Strain elastogram (measured in %). The largest inclusions are visible but the contrast is unknown

1) The Poisson coefficient  $\nu$  is taken to be 0.45, and in a first approximation the domain is assumed to be homogeneous with Young's modulus equal to 1.

2) The boundary conditions are not exactly known, but reconstructed using an efficient implementation of Gauss-Newton algorithm similar to the one explained above (but simpler) : we look for Dirichlet conditions on the inner boundary, and Neumann conditions on the outer boundary.

3) Once the boundary conditions are estimated, algorithm 1 is applied to estimate the relative Young's modulus distribution. Indeed, a Tikhonov regularization term is added to the cost functional :  $J(E) = \frac{1}{2} \|F(E)\|^2 + \alpha \|E\|^2$ .

The results are shown in fig.3. We can distinguish four among the inclusions, the other two inclusions are smaller and do not appear on our results. However, the va-

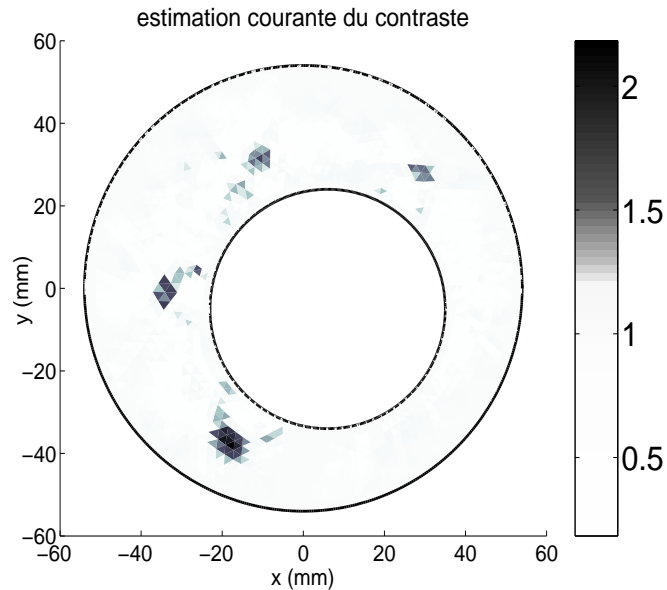


**Figure 3.** *Young's modulus contrast estimation*

lues obtained for the Young's modulus contrast have not been checked by independent measurement. Numerical experiments suggest that the value of the contrast is underestimated.

## 5. Conclusion

We presented in this paper an implementation of Gauss-Newton algorithm that requires little memory and few computations. As an application, this implementation has been applied to the problem of relative Young's modulus identification on experimental data.

## 6. Bibliographie

- Catheline S., Wu F., Fink M., « A solution to diffraction biases in sonoelasticity : the acoustic impulse technique », *J.Acoust.Soc.Am*, vol. 105, p. 2941-2950, 1999.
- Doyley M., Meaney P., Bamber J., « Evaluation of an iterative reconstruction method for quantitative elastography », *Phys.Med.Biol*, vol. 45, p. 1521-1540, 2000.
- Doyley M., Srinivasan S., Pendergrass S., Wu Z., Ophir J., « Comparative evaluation of strain-based and model-based modulus elastography », *Ultrasound Med.Biol.*, vol. 31, p. 787-802, 2005.

- Gao L., Parker K., Alam S., « Sonoelasticity imaging : theory and experimental verification », *J.Acoust.Soc.Am*, vol. 97, p. 3875-3880, 1995.
- Griewank A., *Evaluating derivatives : principles and techniques of algorithmic differentiation*, SIAM, 2000.
- Kallel F., Bertrand M., « Tissue elasticity reconstruction using linear perturbation method », *IEEE Trans.Med.Imaging*, vol. 15, p. 299-313, 1996.
- Kirsch A., *An introduction to the mathematical theory of inverse problems*, Springer, 1996.
- Krouskop T., Wheeler T., Kallel F., Garra B., Hall T., « The elastic moduli of breast and prostate tissues under compression », *Ultrasonic imaging*, vol. 20, p. 260-274, 1998.
- Ophir J., Alam S., Garra B., Kallel F., Konofagou E., Krouskop T., Merritt C., Righetti R., Souchon R., Srinivasan S., Varghese T., « Elastography : Imaging the Elastic Properties of Soft Tissues with Ultrasound », *J.Med.Ultrasonics*, vol. 29, p. 155-171, 2002.
- Ophir J., Cespedes I., Ponnekanti H., Yazdi Y., Li X., « Elastography : a quantitative method for imaging the elasticity of biological tissues », *Ultrasonic imaging*, vol. 13, p. 111-134, 1991.
- Souchon R., Rouvière O., Gelet A., Detti V., Srinivasan S., Ophir J., Chapelon J., « Visualisation of HIFU lesions using elastography of the human prostate in vivo : preliminary results », *Ultrasound Med.Biol.*, vol. 29, n° 7, p. 1007-1015, 2003.
- Souchon R., Soualmi L., Bertrand M., Chapelon J., Kallel F., Ophir J., « Ultrasonic elastography using sector scan imaging and a radial compression », *Ultrasonics*, vol. 40, n° 1-8, p. 867-871, 2002.